

EXPERIMENTAL STUDY ON THE SEISMIC BEHAVIOUR
OF MULTISTORY PRECAST LARGE PANEL
RESIDENTIAL BUILDINGS

Chu Youlin (I)
Liu Yinsheng (II)
Chen Rui (II)
Guan Qixun (II)
Shou Guang (II)
Presenting Author: Chu Youlin

ABSTRACT

This paper presents the study of an eight-storied model test analogous to multistory residential buildings with precast large panels under static and dynamic horizontal loading. The test results show that the stress distribution within the structure and its rigidity are significantly influenced by horizontal and vertical joints between the panels. Analysis of the stability, ductility, and damping coefficient of the designed model verifies that multistory precast panel buildings of same construction have adequate behaviour of earthquake resistance.

INTRODUCTION

In recent years, some 12-storied precast large panel buildings had been constructed in Beijing. In order to verify its aseismic reliability, an 8-storied model test had been carried out to investigate the strength, aseismic behaviour of the structure. Individual tests for horizontal and vertical shear key joints used in actual buildings were also made to study the shear strength, failure modality and constructional details systematically. In this paper, only the model test results are introduced.

MODEL DESIGN

Owing to the restriction of equipments, 8-storied model was designed to simulate the twelve storied precast large panel buildings. The linear scale between the model and prototype is $1/5$ (Fig1-2). Wall panels were made of reinforced microconcrete whose ultimate compressive strength is 200 kg/cm^2 (Fig4-5). An equivalent thickness of 3.4cm solid wall was used for the exterior panels to simulate the sandwich panels of 28cm thickness (Fig3). The cast-in-place top floor designed for setting exciter is 8cm thick. The construction of joints between wall panels and floors are similar to the prototype structure. The horizontal joint were constructed with welded rebars and deep groove shear keys, and the vertical joints with overlapping steel links and shallow groove shear keys. All joints were

(I) Senior Engineer, Beijing Institute of Architectural Design.

(II) Engineer, Beijing Institute of Architectural Design.

packed with cast-in-place concrete (Fig 6).

In order to obtain the same compressive stresses in walls under vertical loading as the prototype structure, some weights were superimposed on each floor of the model.

TEST PROGRAM

The horizontal static loads were applied at stories no.2,4,6,8 by a hydraulic jack with vertical distribution beams to distribute horizontal loads to each floor proportioning to its height. At the top floor of the model a CS46-2 exciter was used for dynamic test. The static and dynamic tests were interchanged in the whole test program as shown in fig(7).

The horizontal displacement of floor, the relative displacements of joints, and the stress of reinforcements at different parts were measured in the tests.

STATIC TEST RESULTS

1. Fig(8) shows the load-displacement relationships of the model at the top floor. When the horizontal loading attains 8.5 tons, yielding of outmost vertical steel at the bottom floor of the model occurs. Table 1. shows the horizontal displacement of each floor at various loading. The flexural rigidity of the model degenerates gradually under cyclic loading, rapid degradation is observed after 9 tons loading.

2. The stress of vertical steels (measured points shown in fig 9) at the bottom of the east wall are shown in Table 2. Tensile stresses occur in the wall piers both on the tension and compression side of model, it explains the integrative flexural effect on the wall piers, the precast panel wall assemblage acts as a coupled shear wall. At the failure of the model the steels of wall pier on tension side break-off, while on the

Horizontal displacement of each floor under static loading. (mm)
Table 1.

| Direction of loading | story no | Horizontal load(tons) | | | |
|--|----------|------------------------|--------------------|--------------------|-------|
| | | 3 | 7 | 9 | 12 |
| S -N | 2 | 0.33 | 0.81 | 1.46 | 5.32 |
| | 1 | 0.56 | 3.47 | 4.02 | 12.75 |
| | 6 | 0.60 | 3.50 | 5.62 | 19.73 |
| | 8 | 1.48 | 1.60 | 7.44 | 24.08 |
| N -S | 2 | | 0.81 | 1.57 | 5.37 |
| | 1 | | 3.43 | 4.16 | 12.17 |
| | 6 | | 3.73 | 6.01 | 18.37 |
| | 8 | | 1.27 | 7.53 | 23.09 |
| effective rigidity(t · m ³) | | 3.74×10^4 | 2.93×10^4 | 2.22×10^4 | |

compression side, the stresses of steels maintained nearly in the yielding state. It explains that the strength of connecting beams between piers are adequate to transfer shears.

The horizontal load-bearing capacity of the model depends mainly on the axial strength of the piers, with little effect of individual bending.

3. The plastic region of the model under collapse load (12 tons) ranges over three stories, the failure mode illustrates the behaviour of a

ductile structure.

Table 2.

| Total horizontal Load | Loading direction | measured points | | | | | | | |
|-----------------------|-------------------|-----------------|--------|--------|--------|--------|--------|--------|--------|
| | | 13 | 1 | 2 | 3 | 4 | 5 | 6 | 18 |
| 3 | S → N | - 350 | - 247 | 0 | - 69.2 | 217 | - 110 | 99 | 131 |
| | N → S | 330 | 297 | 0 | 158 | - 257 | 100 | - 217 | - 350 |
| 7 | S → N | - 1960 | - 1155 | - 550 | - 515 | | - 600 | 337 | 718 |
| | N → S | 700 | 178 | - 380 | 126 | - 703 | - 10 | - 1495 | - 1185 |
| 9 | S → N | - 2720 | - 1267 | - 1370 | - 326 | 960 | - 910 | 416 | 760 |
| | N → S | 1120 | 59.1 | - 590 | - 535 | - 1366 | - 1370 | - 2195 | - 2170 |
| 12 | S → N | - 1650 | - 1851 | - 2500 | - 571 | 1208 | - 1190 | - 386 | 1270 |
| | N → S | 1190 | - 1059 | - 1650 | 106 | - 2534 | - 682 | - 1821 | - 2350 |

4. The cracking loads of different parts of the model are shown in table (3)

Table 3.

| Cracking position | Connecting beam of transverse wall | Horizontal joint | | Diagonal Cracks of transverse wall | Vertical joints |
|-------------------|------------------------------------|------------------|----------------------------|------------------------------------|-----------------|
| | | transverse wall | exterior longitudinal wall | | |
| Cracking load(t) | 2 — 3 | 6 | 4 | 10 | 8 |

5. The compressibility of the cement mortar layer in horizontal joints under axial load reduces the flexural rigidity of the wall panel. The effective elastic modulus of wall panel may be defined as:

$$E_e = 1 / \left(\frac{1}{E_b} + \frac{\lambda_m}{h} \right)$$

E_b : modulus of elasticity of wall concrete;

λ_m : the total deformability characteristic of the horizontal joints in one story; $\lambda_m = n\lambda_k$

h : story height;

n : number of horizontal joints within one story;

λ_k : deformation of each mortar layer under unit compressive stress.

The values of λ_k given by F.Bljucer's test are shown in table 4.

Table 4.

| Compressive strength of the mortar (kg/cm^2) | 10 | 50 | 100 |
|--|-------------------|---------------------|---------------------|
| λ_k ($\text{cm}/\text{kg}/\text{cm}^2$) | $1 \cdot 10^{-3}$ | $0.5 \cdot 10^{-3}$ | $0.1 \cdot 10^{-3}$ |

In the prototype structure, the thickness of the mortar layer is about 10 mm, story height $h=290\text{cm}$ if we take $E_m=2.6\times 10^5\text{kg-cm}^2$, $\lambda_m=0.4\times 10^{-3}$, then $E_c=0.736 E_m$.

In the model test, the thickness of the mortar layer is about 5mm, $h=58\text{cm}$, λ_m may be taken as 0.2×10^{-3} , then $E_c=0.528 E_m$. It shows that the effect of compressibility of mortar layer is greater than that in prototype structure.

6. Another behaviour of the horizontal joints between wall panels is the shear slip reducing the effective shear modulus of wall.

Let Δ_s be the relative shear deformation between panel walls of adjacent stories due to the slip of horizontal joints under lateral force Q , Δ_G , the shear deformation within each story (Fig 10). The total shear deformation is:

$$\Delta = \Delta_s + \Delta_G = \frac{\mu Qh}{G_e A} \quad G_e = G / \left(1 + \Delta_s \frac{GA}{\mu Qh} \right)$$

where:

G_e : effective story shear modulus;

A : area of wall section;

The average shear slip of the wall joints at first story is shown in fig (11). When the horizontal loading is less than 7 tons, the load-slip relationship is linear. For $Q=7$ tons, $\Delta_s=0.039\text{mm}$.

From the above formula, $G_e=0.37G$

Owing to the simulation of model is based on equal stresses, the effective shear moduli of model and prototype are identical.

7. The stress distribution and rigidity of the walls are also influenced by the shear deformation of vertical joints. We consider that the vertical joints acts as discrete continual connecting beams which have only shear rigidity. In the stress analysis, a story-shear flexibility coefficient φ , defined as a relative slip between two adjacent walls due to unit shear force acted on the joint within one story height is introduced. Test of vertical joints used in the model gives $\varphi=5\times 10^{-5}\text{m/t/story}$.

8. From the analysis of experimental data in elastic range, it is found that:

The flexural rigidity of each wall pier under tension is quite different from that under compression. The effective rigidities are $0.32E I$ and $0.85E I$ for piers under tension and compression respectively. I is the moment inertia of corresponding pier. Considering the low steel stresses measured in the connecting beams, it seems that the flexural rigidities of beams are lower than that given by formula based on elastic theory.

DYNAMIC BEHAVIOUR OF THE MODEL

1. Following the removal of static loading, the dynamic model tests had been carried out with CS46-2 exciter according to the following stage:

I. Elastic stage: After the horizontal static load applied up to 3 tons

II. The elastoplastic stage: After the horizontal static load applied up to 9 tons.

III. After the horizontal static load applied up to 12 tons. The width of cracks is significantly increased and ultimate stress is reached

in vertical steels on tension side of model, to a certain extent, the structure still retains the behaviour of restoration.

IV. After the horizontal load applied to 13 tons. The vertical steels on tension side are broken off.

Table 5 shows the results of dynamic tests of the model. Following the progression of dynamic tests in stages, the natural frequency of the model decreases significantly, but the damping coefficient increases with the degree of destruction of the model.

Table 5

| Test Method | Frequency (HZ) and damping coeff. | Stage | | | |
|---|-----------------------------------|---------|-------|-------|-----------|
| | | I | II | III | IV |
| Microseism | natural frequency | 11 ~ 12 | | | 7.5 ~ 8.0 |
| | damping coeff. | | | | |
| Resonance | natural frequency | 10 | 7.3 | 6.7 | 5.5 |
| | damping coeff. | 0.0625 | 0.12 | 0.127 | |
| Low intensity shock | natural frequency | 10 | 7.7 | | |
| | damping coeff. | 0.087 | 0.110 | | |
| By kolousek's damping vibration formula | damping coefficient | 0.08 | 0.130 | | |

2. Table 6 shows the dynamic horizontal displacements of different stories when the maximum horizontal displacement at the top of model is reached. Since the horizontal harmonic disturbing forces produced by the CS46-2 exciter is very small, we may consider the model as a cantilever beam and obtain the approximate value of dynamic effective elastic flexural rigidity which is greater than the corresponding static effective rigidities as shown in table 4.

3. From the values of acceleration shown in table 6, we may get the inertial shear force and moment at the base of model. By Kolousek's damping vibration formula of cantilever beam, when the harmonic horizontal force is applied at the top, we can calculate the dynamic shears and moments for dynamic rigidities shown in table 6, and various damping coefficients. If the disturbing force is equal to that produced by CS46-2 exciter in magnitude and frequency, and the calculated dynamic shear and moment at the base equal to those inertial forces produced by model test, then the value of damping coefficient used in the calculation is the actual damping coefficient which is listed in table 5.

Table 6

| | | Acceleration (cm sec ²) | Horizontal displacement (mm) | Effective dynamic rigidity (t - m ²) | Magnitude of disturbing force (kg) |
|-------------------------|-----------|--|------------------------------------|--|--|
| I. Elastic range | top floor | 132 | 0.332 | 6.35 × 10 ⁴ | 129 |
| | 6th floor | 72 | 0.182 | | |
| | 1th floor | 61 | 0.182 | | |
| II. Elastoplastic range | top floor | 58.5 | 0.274 | 3.35 × 10 ⁴ | 68,917 |
| | 6th floor | 15 | 0.071 | | |
| | 1th floor | 11.2 | 0.053 | | |

Note: wt. of top floor of model = 2170kg
wt. of other floors of model = 4910kg

CONCLUSIONS

1. The model test proves the use of horizontal joints with welded

vertical rebars and deep groove shear keys and vertical joints with steel links and shallow groove shear keys in large panel buildings provide adequate aseismic behaviour. The deformation of joints causes the decrease of rigidities and increase of damping coefficient. Hence, the large panel structures possess adequate ability of energy dissipation at elastoplastic range to resist earthquake. The ductility factor of the test model is 6.2 and the damping coefficient is about 0.06-0.13 under dynamic test. The structural behaviour can be compared with monolithic shear wall construction.

2. In the whole process of testing, the model acts as a coupled shear wall. The model stands still even when piers on tension side are damaged, it shows that stability, integrity and construction details of the model satisfy aseismic requirement.

REFERENCES

1. F.Bljoger: Nonlinear Concrete Wall Characteristics of Significant Importance in Structural Analysis. ACI. Journal Proceeding Vol.45 No.5 June, 1978.
2. CIRIA Report 45: The Behaviour of Large panel Structures.
3. V.Kolousek: Dynamics of Engineering Structures.

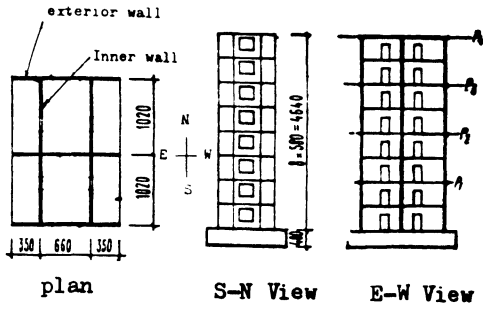


Fig. 1. Plan and elevation of model



Fig. 2. Test model after failure

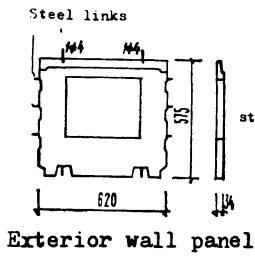


Fig. 3.

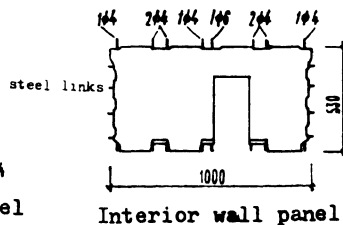


Fig. 4.

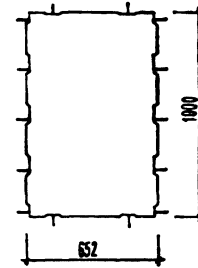
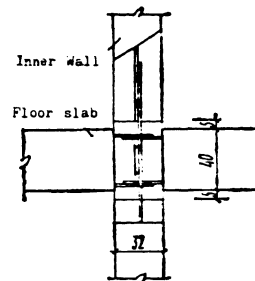
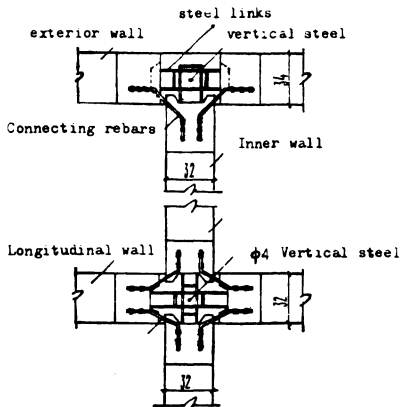
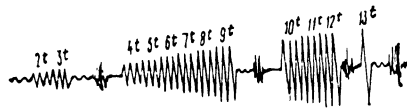


Fig. 5. Floor slab



a. Connection between the walls b. Connection between the wall and floor
Fig. 6.



~~~~~ -Microseism    — — — -Low intensity shock  
 - - - -excitation    ^ ^ ^ -static test

Fig.7 Test program

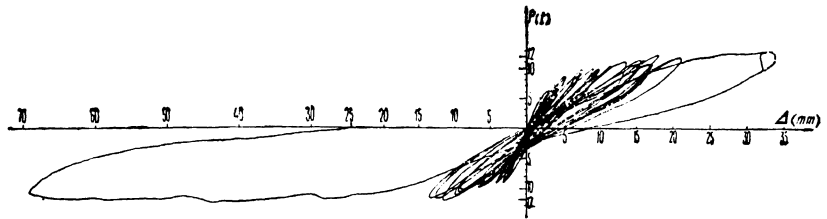


Fig.8.

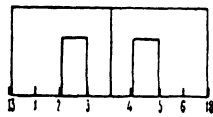


Fig.9.

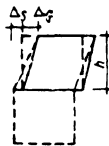


Fig.10.

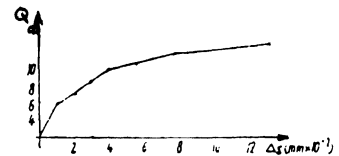


Fig.11.